46TH TURBOMACHINERY & 33RD PUMP SYMPOSIA
HOUSTON, TEXAS | DECEMBER 11-14, 2017
GEORGE R. BROWN CONVENTION CENTER

FORCED RESPONSE ANALYSIS IN A FULL-SCALE MULTISTAGE CENTRIFUGAL COMPRESSOR: IMPELLER VIBRATION PREDICTION AND VALIDATION

Dr. Lorenzo Toni
Lead Engineer
GE Oil & Gas – Nuovo Pignone
Florence, Italy

Dr. Alberto Guglielmo
Lead Engineer
GE Oil & Gas – Nuovo Pignone
Florence, Italy

Dr. François Moyroud
Senior Engineer
GE Oil & Gas – Thermodyn
Le Creusot, France

Dr. Giuseppe Gatta
Senior Engineer
GE Oil & Gas – Nuovo Pignone
Florence, Italy

Dr. Dante Tommaso Rubino
Engineering Manager
GE Oil & Gas – Nuovo Pignone
Florence, Italy

Giacomo Scarabello
Test Engineer
GE Oil & Gas – Nuovo Pignone
Florence, Italy

Lorenzo Toni is a Lead Engineer within the Compressors and Expanders New Product Introduction (NPI) Team at GE Oil & Gas. His responsibilities include the centrifugal compressors aerodynamic design, unsteady aerodynamics and aeromechanic modelling and analysis. Lorenzo joined GE in 2009 as a Test and Data Analysis Engineer and then moved to his present position. He received an M.S. degree in Mechanical Engineering from the Florence University in 2005 and earned a PhD in Energetics from the same University in 2009, with a doctoral research in the area of heat transfer and advanced cooling systems design for combustor liners, turbine endwalls and blades. He is the author or co-author of several technical papers in the field of turbomachinery.

Alberto Guglielmo is a Design Engineer within the Compressors and Expanders New Product Introduction (NPI) Team at GE Oil & Gas. He received his M.Sc. in Mechanical Engineering from the University of Pisa in 2004 and a PhD degree in Mechanical Engineering from the University of Pisa in 2008. He joined GE Oil & Gas in the 2008 working for Requisition Team for centrifugal compressor and in 2011 he has moved to his current position as part of the NPI Team. He has been involved into both analytical and experimental structural dynamic and machine design.

François Moyroud is an Engineering Technical Leader at Thermodyn, entity of GE Oil & Gas, in France. He joined the New Product Introduction (NPI) group as Senior Engineer in 2008. His responsibilities cover the aerodynamic performance of low to medium pressure centrifugal compressors, including integrated electric machines, as well as the experimental and numerical validation of the aeromechanical design of new stages. He has been working with Turbomachinery Aeromechanics for 20 years. He holds a PhD from the National Institute of Applied Sciences of Lyon and from the Royal Institute of Technology of Stockholm. He started his career as Research Assistant, and developed numerical methods to predict military and civil aero engine fan blade flutter. He then joined the Aerospace industry in the UK in 2000 where he acted as aeromechanics specialist on military engine development programs until 2007. He is a member of the ASME.

Giuseppe Gatta is a Senior Engineer of the Compressors & Expanders New Product Introduction (NPI) Team within the Turbomachinery & Process Solutions Organization. He has been with GE Oil & Gas since 2010. His main areas of expertise are aeromechanics, structural dynamics and acoustics as well as static analysis and fatigue calculation. He has been dedicated to improving the aeromechanical design of axial compressor blades and centrifugal compressor impellers, holding technical leadership both for numerical and test activities. He capitalizes on Six Sigma concepts, methodologies and tools to improve product quality and competitiveness. Since his studies he has been pursuing increase of predictive capabilities and numerical-test correlation. He received his M.S. degree in Aerospace Engineering from the University of Naples.

D. Tommaso Rubino is currently the Engineering Manager for Aerodynamics within the Centrifugal Compressors and Turboexpanders organization of GE Oil & Gas, in Florence, Italy. His responsibilities include the aerodynamic design and the performance predictability of the GE Oil & Gas turbocompressors and turboexpanders product lines. Dr. Rubino joined GE in 2006 as Design Engineer in Centrifugal Compressor New Product Introduction (NPI) team, then rolling in the Aero team upon creation of the Advanced Technology Organization, where he has been responsible of the aerodynamic design of new stage families for Centrifugal Compressors. Mr. Rubino received an M.S. degree in Mechanical Engineering in 2002 and a Ph.D. degree in Mechanical Engineering in 2006 from Politecnico of Bari, and he graduated with honors in the Diploma Course program at the von Karman Institute in 2002.

Giacomo Scarabello is a Test Engineer of the GE Oil & Gas Turbomachinery Laboratory, in Florence, Italy. He is responsible for data acquisition systems setup, software implementation for real time monitoring and post-processing, data analysis in collaboration with the different disciplines. He has been mainly involved in aerodynamic and aeromechanical validation. He joined GE Oil & Gas in 2012, within the Edison Engineering Development Program (EEDP), a technical program for engineering graduates. After concluding the program in 2014 he moved to his current role in the Turbomachinery Laboratory. Giacomo received his M. Sc. degree in Energy Engineering in 2011 from University of Padova.

ABSTRACT

Full aeromechanical validation and forced response analysis are becoming fundamental in the design process of centrifugal compressors, especially for high-speed and high-pressure ratio machines operating at variable speed. Synchronous excitations on impellers, mainly due to the unsteady interactions between structural deflections and stationary row wakes and potential fields, may lead, under critical conditions, to high-cycle fatigue failures.

The present paper focuses on the predictive capability of vibratory response of impellers under resonant conditions. Starting from FE (Finite Element) analysis and CFD (Computational Fluid Dynamics) results, the modal force of impeller is computed and the dynamic stresses are properly scaled. Numerical results are validated against test data obtained through an aeromechanical test campaign performed on full-scale multistage centrifugal compressor equipped with transonic unshrouded impellers. Blade flexural modes and hub disk modes have been thoroughly analyzed both for design and off-design conditions and for different pressure levels. The good level of agreement obtained allows deriving, in a purely numerical way, a reliable representation of the Goodman diagrams for the selected mode shapes.

This work confirms the level of maturity and accuracy of the prediction of forced response for open impellers, which is fundamental to ensure reliability and avoid mechanical failure.

INTRODUCTION

This paper represents the follow-up and completion of the paper presented at the TPS2016 by Toni et al. (2016). The tested compressor, instrumentation setup and partial test results together with prediction of aerodynamic damping have been published therein. Here, a further step is presented and extensively discussed, namely the prediction of forced response.

Due to the inherent complexity of the required calculation and the uncertainty connected to it, verification of forced response for a rotating turbomachinery component was usually considered only after a component test for verification, or within a classical root cause analysis (RCA). With this work, it will be shown that Forced Response Assessment (FRA) has reached a level of maturity at the authors' company such that it can be used as a standard procedure during conceptual and detailed design phases of new centrifugal compressor components. This makes the whole process much more robust and effective. In this case, indeed, the analyst can foresee possible design robustness issues and introduce significant modifications with low impact on schedule and cost. In order to be effective, FRA procedure needs to be fully integrated in the design process, so that the designer is able to estimate component vibratory response levels for the different operating conditions and the entire speed range. In other words, through forced response assessment the analyst can virtually perform a comprehensive series of tests in the effort to limit as much as possible the real experimental test campaign needed to validate the design itself.

A reliable prediction of vibratory stresses is fundamentally based on two parallel processes: 1) the calculation of damping characteristics associated with a specified component vibration shape at specified machine operating conditions; 2) the computation of the so called modal work by coupling of excitation forces (i.e. unsteady pressure fields) and structural deflections.

The total damping of centrifugal compressor impellers is "practically" coincident with the aerodynamic damping due to the surrounding flow, and this parameter is extremely important. The approach and software tools used to evaluate the aerodynamic damping of open impellers and their related validation have already been illustrated by the authors in the afore-mentioned paper. Instead, this paper focuses on the whole FRA process which incorporates the aerodynamic damping computation as a crucial step.

The exciting forces generated by upstream and downstream stator components are computed through Computational Fluid Dynamics (CFD) analysis: the outcome of this calculation consists of unsteady pressures defined as a function of frequency. In parallel, structural deflections are determined through a pre-stressed modal analysis. The structural mode shapes are then transferred from the Computational Structural Domain (CSD) onto the Computational Aerodynamic Domain (CAD) and combined with the pressure distribution over the entire aerodynamic surface in order to evaluate the modal work done on the rotating component. Modal work and damping values are then inserted in a classical single-degree-of-freedom (SDOF) formulation to estimate the stress level associated to a specific resonant condition and populate a classic Goodman diagram which allows the identification of the most stressed areas on the component under assessment.

In the work described in this paper, the procedure is applied to an open impeller of a three-section full scale High Pressure Ratio Compressor (HPRC) designed at the authors' company and fully validated through an extensive test campaign carried out in 2015. The FRA results obtained on two disk modes and one blade mode are presented and discussed in detail. The predicted response levels are close to experimental measurements. Moreover, stress level trends obtained as a function of inlet density are discussed, which are useful to extrapolate results at inlet pressures in operation much higher than those normally achievable in a test. Finally, both design and off-design operating conditions have been considered and the tested trends are correctly captured. The demonstrated good level of accuracy allowed deriving in a purely numerical way a reliable representation of the Goodman diagrams for the selected mode shapes.

NUMERICAL METHODOLOGY

The CFD analysis has been performed using a proprietary Reynolds Averaged Navier-Stokes flow solver which is routinely used in performance predictions as part of the design process; a detailed description of the solver may be found in Holmes et al. (1997), whereas examples of its application and validation for centrifugal compressors are reported in Guidotti et al. (2011), Satish et al. (2013) and Guidotti et al. (2014).

Damping Computation

The numerical method for aerodynamic damping computation is described in Toni et al. (2016) and it will be briefly summarized here. A time-linearized Navier–Stokes method is used to predict the aerodynamic damping, where the perturbations to the steady base flow arising from the impeller blade and hub motion are assumed to be small. The steady flow around a periodic sector of the impeller is first modeled. Then, the modal displacements from a finite element model of the structure are mapped on to the CFD grid as a boundary condition to the linearized Navier-Stokes solver and the unsteady pressures resulting from the blade motion are used to compute an aerodynamic work per cycle on the vibrating airfoil. The aerodynamic work is defined as the work removed by the fluid from the vibrating impeller over a cycle of vibration: if the work is positive, the fluid is removing energy from the impeller motion, and it is considered stabilizing, on the contrary, if the work is negative, the fluid is adding energy to the motion and it is considered destabilizing. The aerodynamic work may be converted into an equivalent aerodynamic damping, using the frequency and modal mass associated with the vibration mode. Phase lagged boundary conditions are applied on the periodic surfaces of the model and non-reflecting boundary conditions are applied at the inlet and exit boundaries to minimize pressure wave reflections.

Modal Force Computation

The first step for modal force computation has been the analysis of the impeller aerodynamic response to the inlet distortions: an unsteady CFD analysis is then performed and the unsteady pressure fields at the desired frequencies are extracted. Based on the experience gained so far by the authors, see Toni et al. (2017), non-linear unsteady computations are preferred with respect to time-linearized approaches. The analysis domain included a full annulus impeller and the vaneless diffuser; the upstream flow-path extends up to a surface where the inlet distortion boundary condition, coming from a separate analysis, is applied.

The resulting unsteady pressure field at the frequency of interest is projected onto a basis of orthogonal vectors consisting of a set of natural mode shapes of the impeller. Like for the aerodynamic damping computation, the mode shapes are interpolated onto the CFD grid that is generally finer than the FEA grid on the impeller surface; see also Moyroud et al. (2000).

For a given combination of an impeller mode shape and the unsteady pressure field at a given excitation frequency, the modal force is a complex valued scalar quantity defined as follows:

$$F_{modal} = \left| \Phi^{t} F \right| \tag{1}$$

Where Φ^t is the transpose of the mode shape vector and F represents the unsteady aerodynamic loads in complex form resulting from the surface integration of frequency domain unsteady pressure perturbations on the impeller walls at the excitation frequency of interest (or source of excitation). Generally, the mode shapes are mass normalized and therefore the corresponding modal response displacements or participation factors can be calculated as follows:

$$d_{modal}(\omega_e) = \frac{F_{modal}}{\sqrt{\left(\omega_{modal}^2 - \omega_e^2\right)^2 + \left(\omega_{modal}\omega_e / Q_{modal}\right)^2}} \tag{2}$$

Where $Q_{modal}=1/(2\zeta)$ is the amplification factor calculated from the aero-mechanical modal damping ζ, and ω_{modal} is the natural angular frequency of the impeller mode. Under resonance conditions, the single degree of freedom modal participation factor may be computed:

$$d_{modal}(\omega_e = \omega_{modal}) = \frac{F_{modal} Q_{modal}}{\omega_{modal}^2} \tag{3}$$

It is worth highlighting that aero-mechanical damping includes all the source of damping: in general, it is considered as the sum of material, mechanical and aerodynamic damping. Mechanical damping (or friction damping) is commonly neglected for impellers; hence aeromechanical damping is expressed as the sum of pressure dependent (or better, density dependent) aerodynamic damping and the pressure independent, though mode shape related, material damping; see also Kammerer and Abhari (2009).

$$\zeta_{modal}(\rho) = \zeta_{mat} + \zeta_{aero}(\rho) \tag{4}$$

Then, using the modal participation factor to scale the modal stresses σ_{modal}, the physical alternating stresses σ_{phys} at any node of the FE model can be expressed as:

$$\sigma_{phys} = d_{modal} \cdot k_v \cdot \sigma_{modal} \tag{5}$$

where k_v is a factor introduced to take into account blade-to-blade or sector-to-sector variability due to the manufacturing and balancing processes, or other uncertainties in the prediction process.

EXPERIMENTAL CAMPAIGN

Test Bench and Instrumentation

Test bench and instrumentation are deeply discussed in the cited work by Toni et al. (2016); some essential details are anyway given in the present chapter.

The HPRC prototype test has been performed on a permanent test bench which consists of three independent gas loops, an auxiliary system (lube oil, DGS and cooling) and an electric motor driver; see also Falomi et al. (2016). The test bench is equipped with measurement stations at the inlet and delivery of each compression stage. Four temperature and four pressure measurements are performed in these locations. Being the three gas loops independent, mass flow measurements are performed at inlet and outlet of each compression stage. Regarding aeromechanics measurements, the strain gauges used for validation are positioned on the main walls of open impeller at main blades, splitter blades and disk; as shown in Figure 1. Strain gauge signals are transmitted by a telemetry system that consists of a rotating unit and a stationary unit. The rotating unit is equipped with a miniaturized sensor signal amplifier, A/D conversion module and a radio transmitter, whereas the stationary unit includes an antenna and D/A conversion module. The telemetry output signal is then acquired by a NI PXI-1044 chassis equipped with NI PXI-4472 boards. The boards AC coupling was selected to filter out the low frequency component of the strain. The -3dB cutoff frequency for this filter is 3.4 Hz. The system is equipped with 16 channels used for monitoring the two impellers. A LabVIEW based software communicates to the NI PXI system to acquire and record data at high frequency. Each impeller is instrumented with 8 strain gages distributed in 4 locations for 2 different cyclic sectors. Two strain gages are positioned at main blade, one at splitter blades and one at disk.

Strain gauge position and orientation are optimized by avoiding sensor placement in areas of high stress gradient. This arrangement allows good observability of the selected set of mode shapes as well as providing robustness of the measurements. The quality of strain gauge positioning is expressed in terms of mode sensitivity ratio and strain gradient. The mode sensitivity ratio is defined as the ratio of the strain measured at strain gauge position versus the maximum stress for an arbitrary scale factor of the mode shape. The strain gradient is defined as the ratio between the gradient of the strain in the direction of measurement versus the average strain. The best practice for strain gauge positioning requires a minimum value for sensitivity and a low local stress gradient to minimize the measurement error due to sensor position installation tolerances.

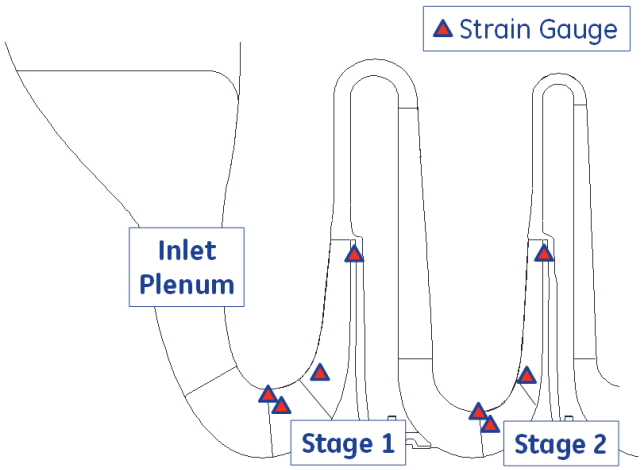

Figure 1 – Schematic of the Strain Gauges (Triangles) on the Open Impellers of Full Scale Compressor

Test Methodology and Post-Processing

During the aeromechanic test, the compressor speed is continuously ramped up from Minimum Operating Speed (MOS) to Maximum Continuous Speed (MCS) to cover the entire design space of the impellers. During a speed ramp, the impeller is subjected to a multi tone sine sweep excitation generated by the aerodynamic drivers existing in the machine.

Impeller vibrations are continuously measured and recorded with a sampling rate of 51 kSample/s. The signals in time domain are divided into a sequence of windows and converted into the frequency domain through FFT analysis. The spectrum sequence is reported in cascade in a waterfall diagram. The vibration amplitudes at different engine orders are extracted and the experimental Campbell diagrams for all strain gauges are monitored. The acceleration ratio of the machine during each speed ramp is small enough to ensure a pseudo stationary signal with limited frequency variation inside each window. The time length of the windows used for the FFT analysis was optimized to be able to analyze all frequency responses with enough data points to accurately reconstruct the resonance in terms of amplitude, frequency and damping factor.

Figure 2 shows the waterfall and the Campbell diagram for a typical speed ramp up: frequency is represented as a function of shaft rotational speed, whereas the fan lines are the so-called engine orders (EO), that is to say running frequency harmonics. The excitation of structural mode is highlighted by a frequency modulation of the synchronous forced response in the Campbell diagram and by the presence of random response not tracked with the speed in the waterfall diagram. The Campbell plot is experimentally obtained from the output of consecutive FFT computations. For this reason, the frequency of each Campbell point is associated to the discrete spectral lines. The distance in the frequency domain between consecutive spectral lines is fixed and defined by the frequency resolution of the FFT analysis. To improve the accuracy of the data, the frequency of the Campbell points is corrected, considering the instantaneous shaft speed and the EO at which the resonance is occurring. Figure 3a shows the Campbell Plot before the frequency correction. Each point is the result of the FFT analysis during the motor ramp up. The distance in the horizontal axis is given by the speed increase between consecutive FFT analyses. The distance on the frequency domain is determined by the resolution of FFT analysis. Figure 3b shows how the frequency of each Campbell Point is corrected. The corrected frequency will be the one of the EO of pertinence at the speed where the Campbell point was recorded. The result of the correction is shown in Figure 3c.

The amplitude response of each strain gauge is then fitted with a Single Degree Of Freedom (SDOF) numerical model and the modal damping (aero + mechanical) is obtained. Figure 4 shows an example of curve fitting (red curve) applied to experimental data (yellow dots) for a specific resonant crossing.

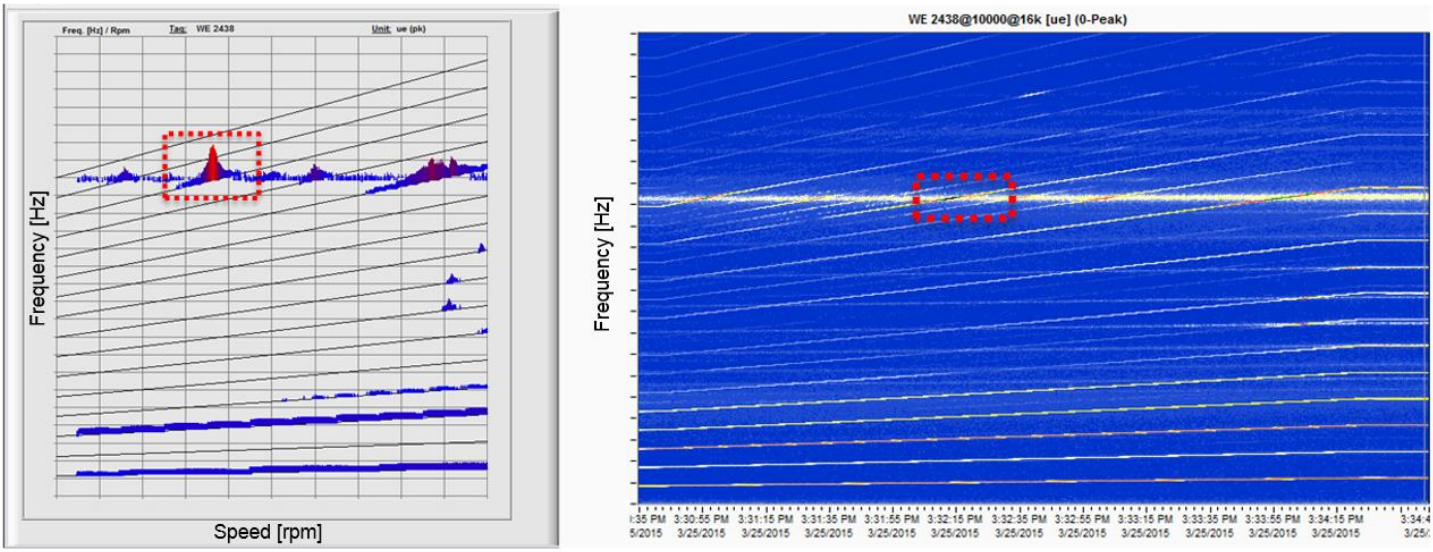

Figure 2 – Waterfall Diagram and Experimental Campbell Diagram

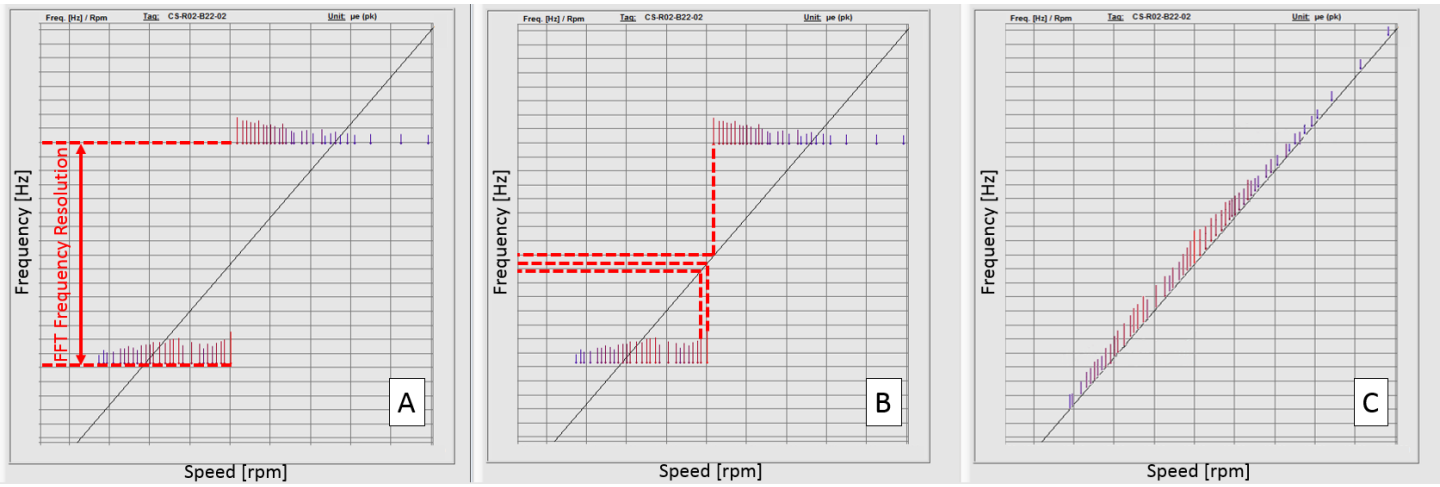

Figure 3 - Frequency Correction along the Engine Order Line

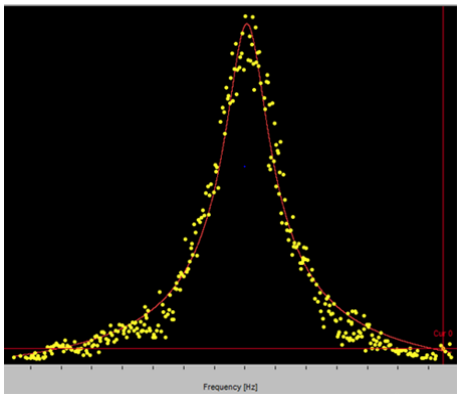

Figure 4 – SDOF Response Fitting at Strain Gauge

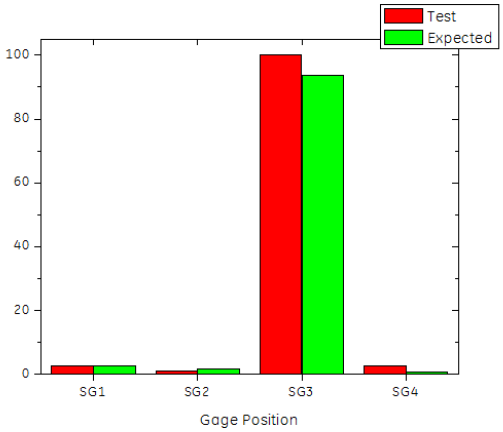

Figure 5 – Matching Between Numerical and Experimental Mode Shape

A simplified Modal Assurance Criterion (MAC) is used to identify the excited mode such that the contribution of the modes out of resonance is assumed negligible (SDOF approach). The amplitude ratio between different strain gauges calculated with Finite Element (FE) model is compared with the measured value and the match is evaluated. Figure 5 shows a comparison of numerical and experimental strain ratios for a pure blade bending mode.

By means of the transfer functions derived from a finite element model, the strain measured at the SG location is related to the one at the impeller critical point on the Goodman diagram. 100% scope limit is obtained when the maximum allowable strain at the critical point in the Goodman diagram is reached: see Figure 6. When the measured strain gauge ratios and FE modal shapes are consistent, strain amplitudes at resonance can be used to scale the Goodman diagram and to perform a fatigue assessment of the impeller.

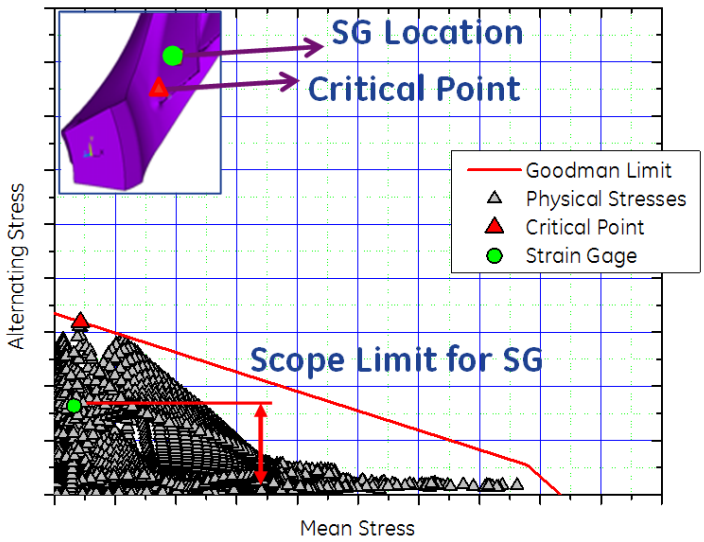

Figure 6 – Scope Limit Definition at Strain Gauge Location

Due to the low observability of the system imposed by available channels for SGs in the telemetry system (only two impellers sectors are instrumented) the measured response level is multiplied by a factor called "blade to blade variability", here denoted with k_v. The physics behind the use of this multiplying factor is that all the blades don't show the same response level due to a partially break of impeller cyclic symmetry.

In principle in a perfect cyclic structure the modes appear in pairs as twin modes with the same frequency and shapes but rotated 90 deg. Each mode or any linear combination of them represents a natural deflection of the structure for the given frequency. Therefore, a cyclic structure subjected to a travelling wave excitation (i.e. potential field in rotating frame) responds with a similar travelling wave and all sectors are subjected to the same vibration cycle.

When the cyclic symmetry is broken the two modes become separate in frequency and the structure response subjected to a travelling wave tends to be a stationary wave with different amplitude among the sectors. The points with a maximum deflection and nodal diameters doesn't travel anymore over the impeller during the rotation. The limit case of this situation is a heavily broken cyclic symmetry where more than two modes are present with associated mode shapes that involves only a portion of structure. Without entering in the details of this behavior called "mistuning", a practical way to consider the different response of the blade is the use of k_v.

The proper value of k_v to be used in the post processing of test data depends on the impeller manufacturing technology and the number of sensors installed. The lower the number of instrumented sectors is, the higher will be the k_v to be used to capture the maximum response over the impeller.

An alternative way to quantify the effect of blade to blade variability is the measure of different dynamic behavior before the test. Usually during the preparation of impeller aeromechanic test an experimental modal analysis test is performed to confirm the frequency position and shapes of modes under investigation. The position of measurement points and excitation locations are optimized to guarantee the observability of the structure with a minimum set of installed sensors. The test setup can be modified adding an excitation point per blade and measuring the response at same location. This procedure is very easy if the test is carried out with a roving hammer and a laser vibrometer to avoid errors introduced by mass modification due to sensor movements. A series of "collocated" transfer function is measured and the dynamic stiffness of each blade is referred to the one having an instrumented sector with gages, and the amplitude ratio is calculated. The k_v is defined as the maximum of the blade amplitude ratio over all sectors. Figure 7 reports the dynamic stiffness of each main blade evaluated at the first flexural mode. A frequency difference of 2% between different blades is measured; a reasonable value of k_v has been obtained and used in the following data reduction. The procedure is repeated also for first flexural mode of splitter blades.

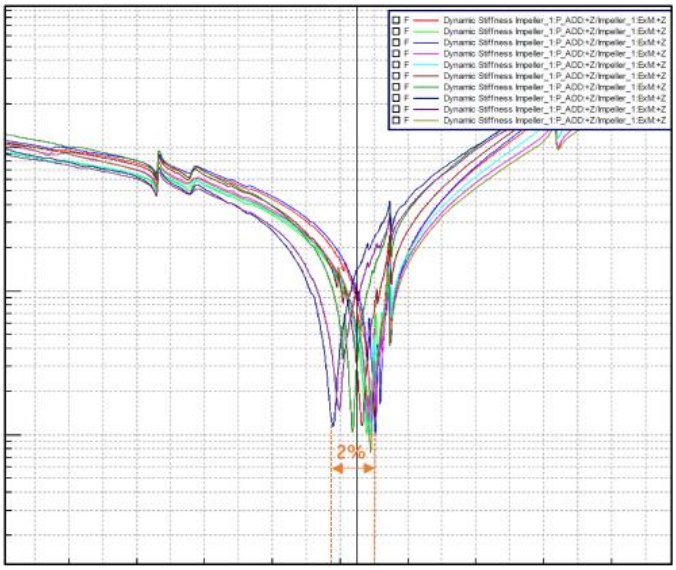

Figure 7 – Blade Dynamic Stiffness for First Flexural Mode

RESULTS AND DISCUSSION

Excitation Source and Resonant Crossings

Inlet distortions coming from the upstream plenum are considered capable of interacting with the downstream impeller up to medium-high order drivers (from 11/Rev to 16/Rev); indeed, see again Toni et al. (2016), inlet plenum flow field contains a wide range of circumferential harmonics that may generate unsteady loading variation though having low magnitude. As an organic completion of previous work, we will focus on vibratory response levels for same mode shapes considered for aerodynamic damping analysis: two modes with high hub disk participation, having 7 and 8 nodal diameters respectively, and a blade first flexural mode (MB 1F), excited by the 14/Rev. These cases were numerically analyzed using the previous approach discussed.

An FEA cyclic symmetric pre-stressed modal analysis was performed on the impeller to obtain impeller natural modes; these results were combined with the synchronous excitation lines to derive the SAFE diagram shown in Figure 8, together with the representation of the mode shapes of interest. Tested impeller has been designed with 22 blades, 11 main blades + 11 splitter blades, thus having 11 periodic sectors. For more details about SAFE diagram representation reader is addressed to Singh et al. (1988).

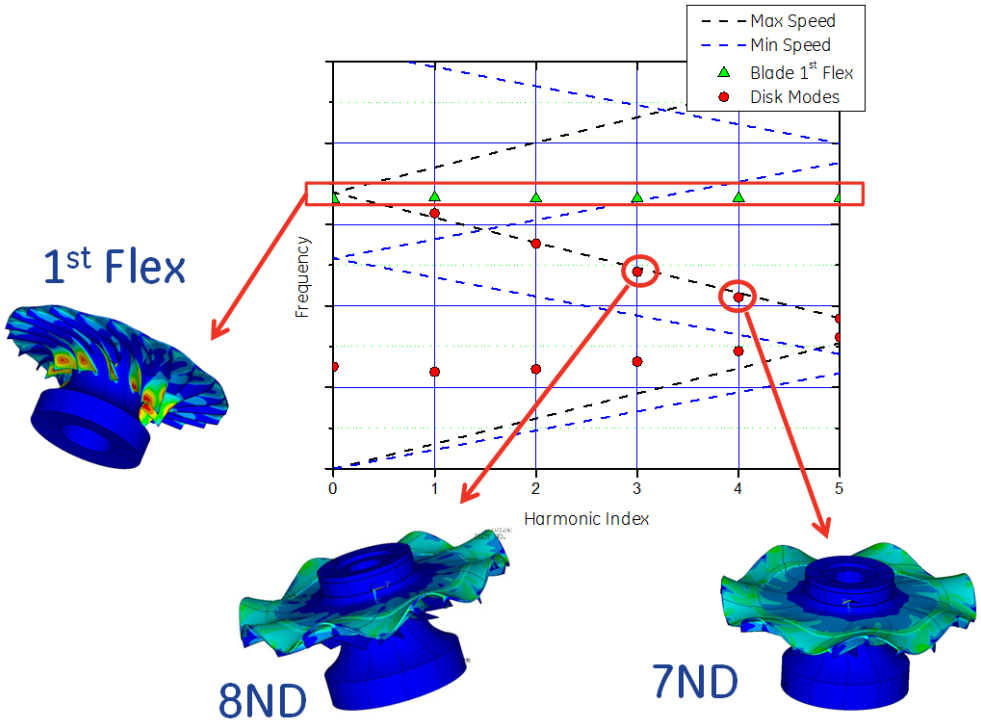

Figure 8 – Interference Diagram

Aerodynamic Damping

Predicted and measured aeromechanic damping values for the resonance crossings analyzed in present paper have been widely discussed and analyzed in the paper by Toni et al. (2016); for readers' convenience, the main results are summarized here. Only the results related to the impeller disk trailing edge mode with 8 nodal diameters are shown, since the general observations may be easily extended to the other ones. Figure 9, left, represents the measured damping values, normalized by an average value, as a function of gas density. As shown, a linear increase of aeromechanic damping with the increasing density has been experimentally verified, thus demonstrating the inertial nature of aerodynamic damping phenomenon; CFD predicts well both trends and absolute values. Figure 9, right, gives an overview, for all the modes that will be considered in present papers, of the measured damping and their respective predicted values for a normalized inlet density of ≈ 6.7-7.0, corresponding to the same gas density level that will be considered for modal force computation. As clearly depicted, a good agreement between test data and prediction has been found.

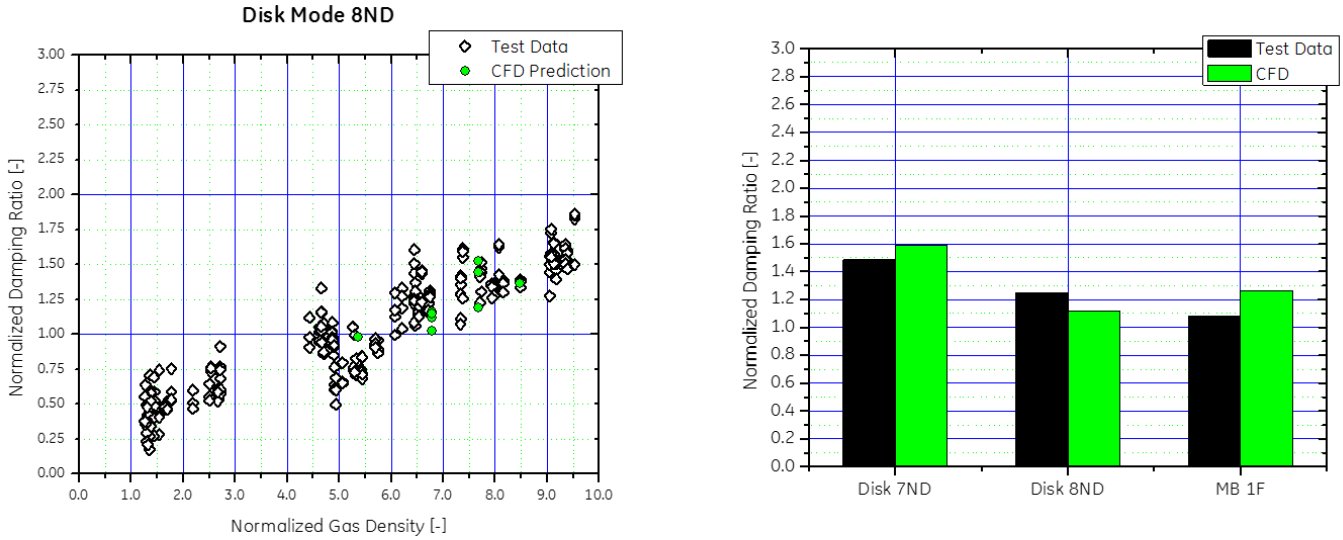

Figure 9 – Normalized Damping vs Density for 8 ND Mode (left); Normalized Damping Summary (right)

Response Levels – CFD Predictions vs Test Measurements

Using the single degree of freedom approach discussed in "Modal Force Computation" section, the alternating stress for each node of the impeller model used for finite element analysis may be expressed as:

$$\sigma_{phys} = \frac{F_{modal} Q_{modal}}{\omega_{modal}^2} \cdot k_v \cdot \sigma_{modal} \tag{6}$$

Response levels, expressed as scope limit percentage; for each mode shape, response level have been normalized using an average value from all positions and operating conditions.

This section represents a precious collection of the most relevant numerical and test data available at the authors' company. The reader will find a considerable amount of data organized in a meaningful series of plots. In some cases, the presented diagrams are nearly self-explaining, nevertheless some comments and considerations are left here to help the reader at interpreting them more quickly. During prototype testing two disk modes (respectively characterized by 7 and 8 NDs) were found out vibrating at high speed along with a blade mode at lower speed, all excited by flow distortions coming from the inlet plenum.

The first set of plots shows the normalized response level as function of a normalized flow coefficient, φ/φ^*, for all mentioned modes. All the available data having a normalized inlet density ranging from approximately 6.7 to 8.4 have been considered: this range has been chosen, since, as it will be more clear later, starting from here the effect of density on response level starts to be less significant, thus meaning that the effects of density and flow rate can be decoupled.

Figure 10 and Figure 11 represent the measured response level as a function of flow rate for disk modes having 7 and 8 NDs. It can be easily concluded that the bigger the flow coefficient is (i.e. the volumetric flow), the higher the response amplitude is and in particular when passing from design flow region to close to choke margin. Indeed, though some spread in data is present, alternating stresses increase by a factor of 2 for 7 ND mode and by a factor of 2 (or higher, since no data at design point are available) for 8 ND mode. Figure 12 shows the same quantities for main blade flexural mode, in this case response level in deep choke was not experimentally measured.

On the same figures the predicted response levels close to design point ($\varphi/\varphi^* \approx 1.1$) and close to choke ($\varphi/\varphi^* \approx 1.3$) are represented in green symbols; a factor k_v, coming from the previously discussed experimental modal analysis, has been used. Numerical predictions have been normalized through the same factor used for measurements.

For both disk modes under analysis, the predicted response level is in a fair good agreement with test data: both absolute values and trends have been obtained. As far as main blade flexural mode is concerned, numerical outcomes may be compared to test data only in design flow region, where a good predictability is demonstrated. Like for the other mode shapes, flexural mode response level at $\varphi/\varphi^* \approx 1.3$ has been computed: in this case, based on predictions, alternating stresses increase by a factor 2.

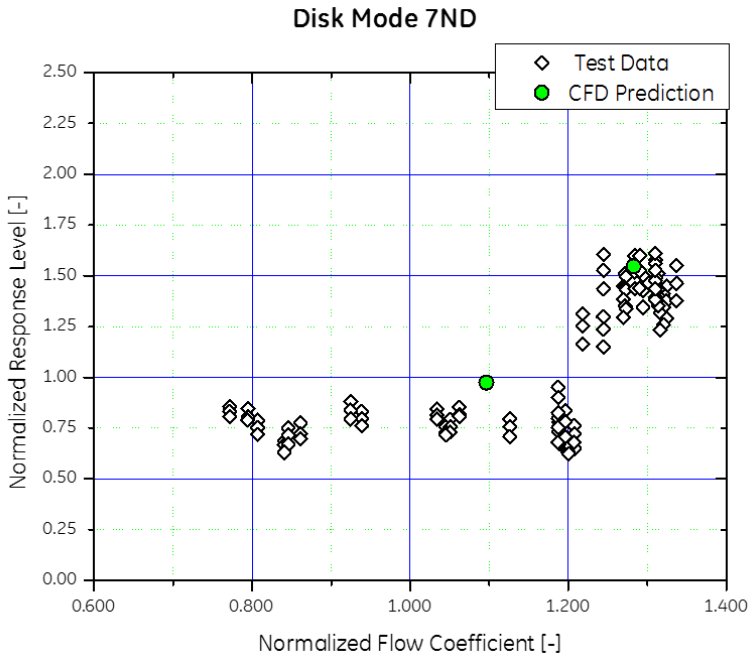

Figure 10 – Disk Mode 7ND: Response Level vs. Flow Coefficient

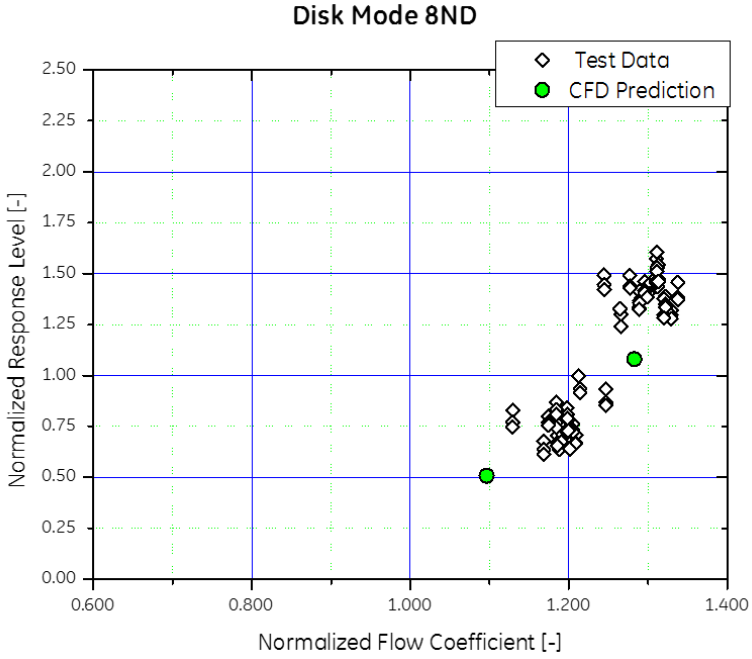

Figure 11 – Disk Mode 8ND: Response Level vs. Flow Coefficient

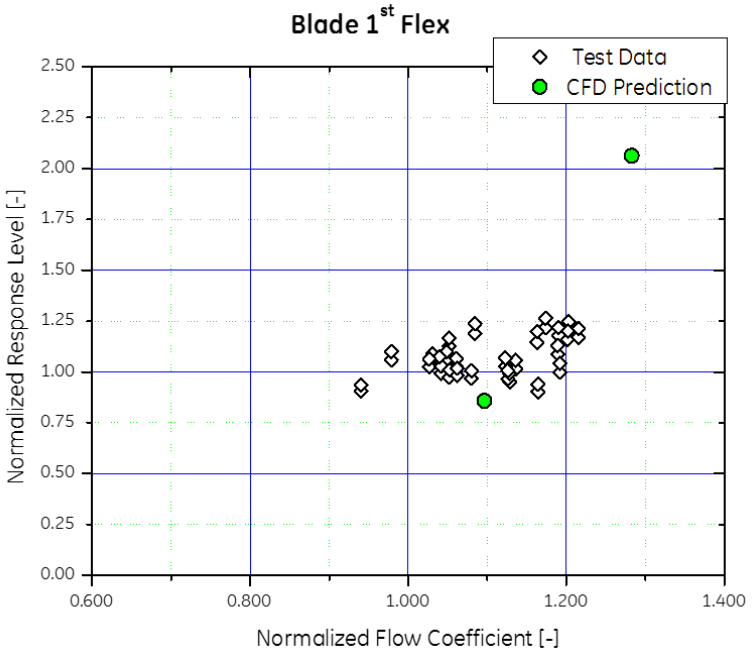

Figure 12 – Blade First Flexural Mode: Response Level vs. Flow Coefficient

Test Data Scaling

The mechanical design of impellers is usually completed with the dynamic response scaling. Usually, due to test bench limitations or limited available power of driver, the aeromechanic test is performed at low inlet pressure and in full speed condition. Therefore, measured dynamic response is scaled with test conditions and generally extrapolated to worst operating conditions of that impeller to verify the structural integrity of the impeller.

A practical parameter to scale the dynamic response is the average density elaborated by the impeller, here denoted with ρ. Without considering any modification generated by a coupling between gas surrounding the impeller and impeller itself, in equation (6), the dependent parameters with operating conditions are the modal force, F_{modal}, and amplification factor, Q_{modal}.

Toni et al. (2016) demonstrated that the modal damping linearly increases with the average gas density elaborated in the impeller. At the same time, the modal force, which is caused by unsteadiness of flow applied to impeller walls, is again proportional to the average gas density. Therefore, the response level can be expressed with a rational polynomial function of first order reported in equation (7).

$$R.L.[\%] = \frac{k_1 \cdot \rho}{k_2 + k_3 \cdot \rho} \tag{7}$$

Equation (7) is positive definite function, uniformly increasing, with an asymptotic value expressed by the ratio k_1/k_3. The coefficients k_2 and k_3 are calculated at first with the fitting of modal damping, then k_1 is obtained through the fitting of measured dynamic response.

An example of test data scaling is reported in Figure 13 for the two disk modes, where a clear asymptotic trend is discovered when the measured response amplitudes are plotted against the inlet density; the asymptotic response levels are obtained with an uncertainty, due to spread in test data, of approximately 5%. The mechanical design of impeller is verified using the asymptotic value of dynamic stress in the Goodman diagram.

Response Levels – CFD Predictions vs Test Measurements

The outcome consists of a stress distribution map over the impeller surfaces through a Goodman diagram like the one represented in Figure 14 for disk mode 8ND. The FE model nodes have been divided in three different groups: hub-side, cavity-side and impeller OD nodes. On average, static stress levels on hub-side result sensibly higher than those on cavity-side. The points with highest dynamic stress levels belong to the external portion of the impeller. To be highlighted that the Goodman line (in black color) has been artificially shifted with respect to its original position to protect intellectual property.

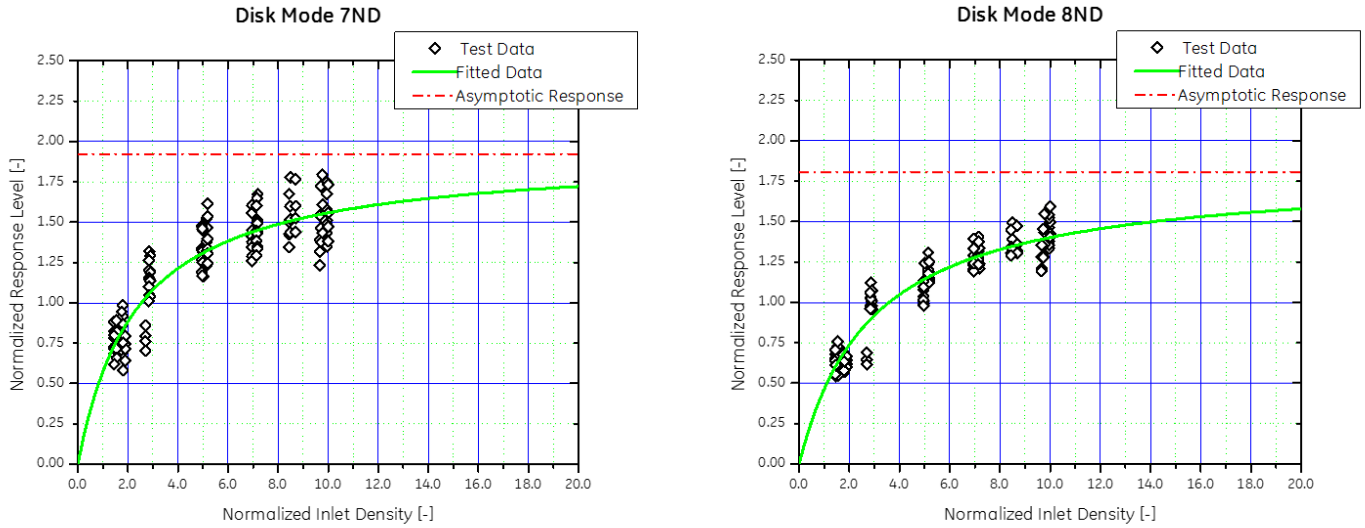

Figure 13 – Response Level vs. Inlet Density: Disk Mode 7ND (left), Disk Mode 8ND (left)

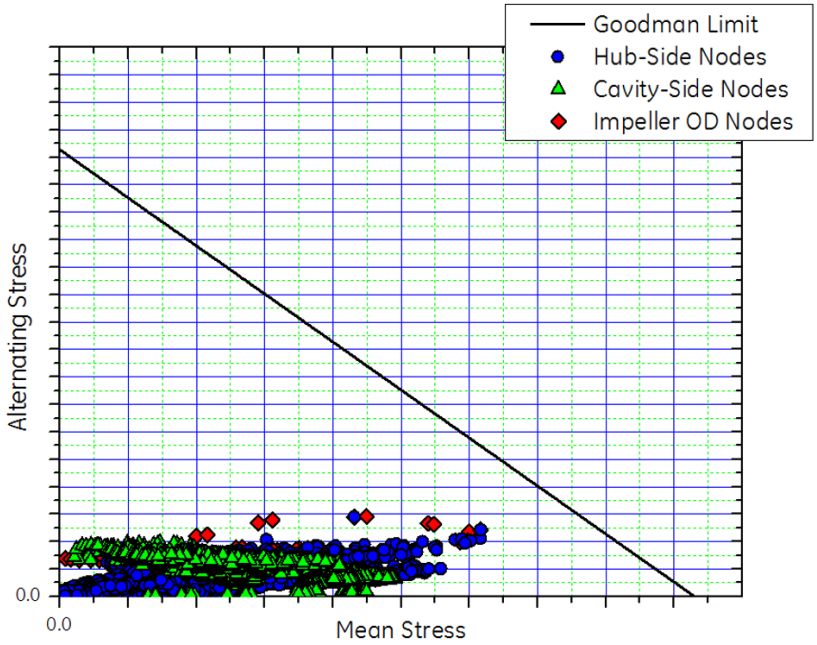

Figure 14 – Numerical Goodman for Disk Mode 8 ND (Goodman Line only for Representation)

CONCLUSIONS

In this paper the verification of forced response prediction vs test results on a full-scale centrifugal compressor impellers is reported and extensively discussed. The test setup included extensive instrumentation of the first two open impellers with strain gauges, allowing detailed measurement of vibratory response and stresses related to different vibration modes. The numerical prediction of the impeller behavior is thoroughly presented. Together with aerodynamic damping prediction, numerical forced response analysis allowed building a "numerical" Goodman diagram.

Three impeller modes are taken into consideration, two disk modes characterized by different nodal diameters and one blade flexural mode. The predicted response matches remarkably well with the test data, demonstrating a significant progress in the prediction capability of aeromechanic phenomena. To this purpose both design and off-design operating conditions have been considered and the test trends are correctly captured.

In summary, this work demonstrates that the predictive capability of forced response for centrifugal compressor impellers has reached a significant level of maturity, and represents today an enabler for mitigating and preventing aeromechanical risk.

NOMENCLATURE

D	= Impeller External Diameter	[m]
F	= Frequency	[Hz]
F	= Aerodynamic Motion Independent Force	[N]
F_{aero}	= Aerodynamic Motion Dependent Force	[N]
F_{modal}	= Aerodynamic Modal Force (Motion Independent)	depends on mode shape normalization
k_v	= Blade to Blade Variability Factor	[-]
N	= Number of Sectors	[-]
P	= Pressure	[Pa]
Q	= Damping Amplification Factor	[-]
Q_{vol}	= Volumetric Flow Rate	[m^3/s]
U	= Peripheral Speed	[m/s]

Greeks

φ	= Flow Coefficient $\frac{4Q_{vol}}{\pi D^2 u}$	[-]
φ*	= Design Flow Coefficient	[-]
Φ	= Mode Shape	depends on normalization
ρ	= Density	[kg/m^3]
σ	= Stress	[MPa]
ζ	= Overall Critical Damping Ratio	[-]
ζ_{aero}	= Aerodynamic Critical Damping Ratio	[-]
ζ_{mat}	= Material Critical Damping Ratio	[-]
Ω	= Frequency	[rad/s]

Acronyms

CAD	= Computational Aerodynamical Domain
CFD	= Computational Fluid Dynamics
CSD	= Computational Structural Domain
EO	= Engine Order
FE	= Finite Elements
FRA	= Forced Response Assessment
IBPA	= Inter Blade Phase Angle
HI	= Harmonic Index
HPRC	= High Pressure Ratio Compressor
MAC	= Modal Assurance Criterion

MCS = Maximum Continuous Speed
MOS = Minimum Operating Speed
Mol. Wt. = Molecular Weight
ND = Nodal Diameter
OEM = Original Equipment Manufacturer
SDOF = Single Degree of Freedom
SG = Strain Gauge

REFERENCES

Falomi, S., Iurisci, G., Fattori, S., Grimaldi, A., Aringhieri, C., Sassanelli, G. And Iannuzzi, G., 2016, "Full Scale Validation of a High Pressure Ratio Centrifugal Compressor," *Proceedings of the 45th Turbomachinery Symposium*, Turbomachinery Laboratory, Texas A&M University, College Station, Texas.

Guidotti, E., Tapinassi, L., Toni, L., Bianchi, L., Gaetani, P., and Persico, G., 2011, "Experimental and Numerical Analysis of the Flow Field in the Impeller of a Centrifugal Compressor Stage at Design Point," ASME Paper GT2011-45036.

Guidotti, E., Toni, L., Rubino, D. T., Tapinassi, L., Naldi, G., Satish, K., and Prasad, S., 2014, "Influence of Cavity Flows Modeling on Centrifugal Compressor Stages Performance Prediction Across Different Flow Coefficient Impellers," ASME Paper GT2014-25830.

Holmes, D.G., Mitchell, B.E., and Lorence, C.B., 1997, "Three Dimensional Linearized Navier-Stokes Calculation for Flutter and Forced Response," ISUAAT Symposium, Sweden.

Kammerer, A., and Abhari, R. S., 2009, "Experimental Study on Impeller Blade Vibration During Resonance Part 2: Blade Damping," *Journal of Engineering for Gas Turbines and Power*, 131 (2), pp. 022509-9.

Moyroud, F., Cosme, N., Jocker, M., Fransson, T. H., Lornage, D., Jacquet G., 2000, "A Fluid-Structure Interfacing Technique for Computational Aeroelatic Simulations," 9th International Symposium on Unsteady Aerodynamics, Aeroacoustics and Aeroelasticity of Turbomachines, Lyon, Sep 2000.

Satish, K., Guidotti, E., Rubino, D. T., Tapinassi, L., and Prasad, S., 2013, "Accuracy of Centrifugal Compressor Stages Performance Prediction by Means of High Fidelity CFD and Validation Using Advanced Aerodynamic Probe," ASME Paper GT2013-95618.

Singh, M. P., Vargo, J. J., Schiffer, D. M. and Dello, J. D., 1988, "Safe Diagram – A Design Reliability Tool for Turbine Blading, *Proceedings of the 17th Turbomachinery Symposium*, Turbomachinery Laboratory, Texas A&M University, College Station, Texas, pp. 93-101.

Toni, L., Moyroud, F., Rubino, D. T., Gatta, G., Guglielmo, A., Ramakrishnan, K., 2016, "Aero-Damping Measurements and Computation in a Full-Scale Multistage Centrifugal Compressor," *Proceedings of the 45th Turbomachinery and 32nd Pump Symposia*, Turbomachinery Laboratory, Texas A&M University, College Station, Texas.

Toni, L., Moyroud, F., Ramakrishnan, K., Michelassi, V., Schurr, E., 2017, "Prediction and Validation of High-Performance Centrifugal Compressor Impeller Forced Response," European Conference on Turbomachinery Fluid dynamics & Thermodynamics, ETC2017-260.

ACKNOWLEDGEMENTS

The authors would like to express their gratitude to General Electric Oil & Gas for its sponsorship of the work herewith presented and the permissions to proceed with its publication. Thanks are due to the Oil & Gas Technology Laboratory (OGTL) and to the Manufacturing String Test Department.

